Semiautomatic determination of the reconstruction volume for real-time freehand 3D ultrasound reconstruction

Article *in* Proceedings of SPIE - The International Society for Optical Engineering · February 2009

DOI: 10.1117/12.811574

CITATIONS
2

READS
21

3 authors:

Yakang Dai
Chinese Academy of Sciences
27 PUBLICATIONS **405** CITATIONS
SEE PROFILE

Jie Tian
Chinese Academy of Sciences
661 PUBLICATIONS **7,114** CITATIONS
SEE PROFILE

Jian Zheng
Suzhou Institute of Biomedical Engineering an…
20 PUBLICATIONS **217** CITATIONS
SEE PROFILE

Semiautomatic Determination of the Reconstruction Volume for Real-time Freehand 3D Ultrasound Reconstruction

Yakang Dai, Jie Tian and Jian Zheng

Medical Image Processing Group, Institute of Automation, Chinese Academy of Sciences, Room 931, No.95 Zhongguancun East Road, Haidian Dist., Beijing 100190, China

ABSTRACT

Freehand 3D ultrasound makes use of a 2D ultrasound system and a position sensor to reconstruct 3D ultrasound images. To achieve real-time reconstruction while acquisition, the reconstruction volume must be determined in advance. In this paper, a novel technique is proposed to address the problem effectively. This technique consists of two steps: the interactive selection of the region of interest (ROI), and the automatic determination of the reconstruction volume. The tracked B-scan is used as a vivid tool to explore the target object. After the decision of the principal directions of the target object, four B-scans are designated to enclose the ROI. The reconstruction volume corresponding to the ROI is then figured out automatically according to the four tracked B-scans. The presented technique can fast predetermine a compact reconstruction volume aligned with the best viewing direction. Furthermore, the technique is convenient for the clinician and comfortable for the patient. The efficient and flexible nature of the technique is demonstrated on a real-time freehand system.

Keywords: Freehand 3D ultrasound, real-time reconstruction, reconstruction volume, ROI

1. INTRODUCTION

3D ultrasound is an important medical imaging modality, and is commonly used in the clinic due to its stereo representation of the target object. There are several methods of performing 3D ultrasound imaging,[1] including direct 3D imaging with a 3D probe, freehand 3D reconstruction with a position sensor, and so on. 3D probes can update volumes in real time. However, they are expensive, and the size or resolution of acquired volumes is limited, which restrict wide uses of 3D probes. The freehand technique uses a conventional 2D ultrasound machine and a position sensor to reconstruct a 3D ultrasound volume: first the receiver of the position sensor is attached to the probe of the 2D ultrasound machine to track the position and orientation of the B-scan image, then a set of B-scan images with the relative positions and orientations are collected and reconstructed to build up the volume. The freehand technique can achieve 3D imaging of a large region. Furthermore, the technique is cheap and flexible. Therefore, freehand 3D ultrasound is frequently used in clinical applications such as neurosurgery.[2,3]

Considering artifacts caused by movement, and time-consuming computation of reconstruction and visualization, conventional freehand technique separates the acquisition, reconstruction, and visualization steps, i.e., performs volume reconstruction after all B-scan images and the relative positions and orientations are acquired, and performs visualization after volume reconstruction. Nevertheless, one pitfall of the separation is that the clinician has to wait a long time to see the reconstruction result before the reconstruction and visualization are finished. Another pitfall is that the clinician can not get real-time feedbacks about the validity of the acquisition, so that the acquisition is highly dependent on experience of the clinician, which may result in discarding the reconstructed volume after visualization. The two disadvantages greatly decrease the efficiency and accuracy of freehand 3D reconstruction. One method of addressing the problems is real-time reconstruction and visualization during acquisition, with which the clinician can know, in real time, which regions of the volume have been reconstructed, and which regions need further reconstruction, so that he can scan interactively to obtain high quality 3D images.

Corresponding author: Jie Tian, E-mail: tian@ieee.org, Tel: 86-10-82628760, Fax: 86-10-62527995, Website: www.mitk.net, www.3dmed.net.

Medical Imaging 2009: Ultrasonic Imaging and Signal Processing, edited by Stephen A. McAleavey, Jan D'hooge
Proc. of SPIE Vol. 7265, 72651E · © 2009 SPIE · CCC code: 1605-7422/09/$18 · doi: 10.1117/12.811574

Some publications have reported systems and techniques for real-time reconstruction and visualization. With an imaging board based on a multimedia video processor, Edwards et al.[4] developed an interactive 3D ultrasound system, which can perform real-time volume reconstruction and visualization during acquisition and operate at 12.5 frames/s. Welch et al.[5] developed a real-time freehand 3D ultrasound system for image-guided surgery. The system allows real-time updates to the scanned volume data as well as the capability to simultaneously display crosses-sections through the volume and a volume-rendered perspective view. Gobbi and Peters[6] described a technique whereby the real-time 3D reconstruction occurs as the data is acquired, where the operator can view the three orthogonal slice views through the reconstructed volume. Their system can reconstruct images cropped from video frames (320×240) at 30 frames/s. Dai et al.[7] implemented real-time reconstruction and visualization during acquisition, and introduced the reconstructed ratio and increased ratio into the real-time reconstruction. The reconstructed volume, reconstructed ratio, and increased ratio are displayed during acquisition, which provides the operator with both qualitative and quantitative feedbacks on acquisition and reconstruction.

To achieve real-time reconstruction during acquisition, the reconstruction volume, including the volume coordinate system (axes and axes origin), voxel size, and volume size, are required before acquisition. Barry et al.[8] used a user-selected key ultrasound frame that is centrally located and depicts a complete cross-section of the target object to define the axes and axes origin of the reconstruction volume. San José-Estépar et al.[9] used Principal Component Analysis (PCA) to select the volume coordinate system and volume size, and proposed a method to determine the voxel size. Nevertheless, the two techniques[8,9] are not suitable for real-time reconstruction, because the reconstruction volume can not be determined before all B-scan images are collected. Gobbi et al.[10] used the extent and voxel spacing of a pre-operative MRI volume to predefine the volume size and voxel size of the reconstruction volume. However, the definition of the volume coordinate system was not described, and it is costly to use a MRI volume to predefine the reconstruction volume. Solberg et al.[11] advised estimating the extent of the reconstruction volume by knowledge of the starting position, movement direction, and type of probe movement if no previous voxel grid can be used for reference. But a detailed method of estimating the extent was not described. The publications[4–7] did not describe details about the predetermination of the reconstruction volume.

To date, a method, which can predetermine the reconstruction volume efficiently and flexibly, has not been described in literature. Motivated by this problem, we develop a novel technique to achieve fast, accurate, and convenient predetermination of the reconstruction volume for real-time reconstruction. The technique comprises two steps: interactive selection of the ROI, and automatic determination of the reconstruction volume. In the first step, four tracked B-scans are designated interactively to surround the ROI, and information of the four designated B-scans are recorded. Then in the second step, the reconstruction volume corresponding to the ROI is determined automatically according to the previously recorded information. In this paper, we describe the semiautomatic technique in detail, and demonstrate its efficiency and flexibility on a custom real-time freehand system.

2. METHODS

2.1 Coordinate Systems

Freehand 3D ultrasound refers to four coordinate systems. As shown in Figure 1, P is the coordinate system attached to each B-scan image. R and T are the coordinate systems of the receiver and transmitter of the position sensor respectively. C is the coordinate system of the reconstruction volume. The transformation from P to C can be written as:[12]

$$\begin{cases} {}^{C}T_{P} = {}^{C}T_{T} \cdot {}^{T}T_{R} \cdot {}^{R}T_{P} \\ {}^{C}X = {}^{C}T_{P} \cdot {}^{P}X, \end{cases} \tag{1}$$

where ${}^{P}X$ is the position of each pixel in P. ${}^{R}T_{P}$, ${}^{T}T_{R}$, ${}^{C}T_{T}$, and ${}^{C}T_{P}$ can be written as a uniform format ${}^{J}T_{I}$, which denotes the transformation from the coordinate system I to the coordinate system J. ${}^{C}X$ is the position of each pixel in C. ${}^{R}T_{P}$ is a constant matrix that is predefined by spatial calibration. ${}^{T}T_{R}$ can be figured out with the six-degree-of-freedom parameters which are read directly from the position sensor. ${}^{C}T_{T}$ can be figured out with the axes and axes origin of the volume coordinate system. The axes, axes origin, voxel size, and volume size are worked out by the two steps that are described in Subsection 2.3 and Subsection 2.4 respectively.

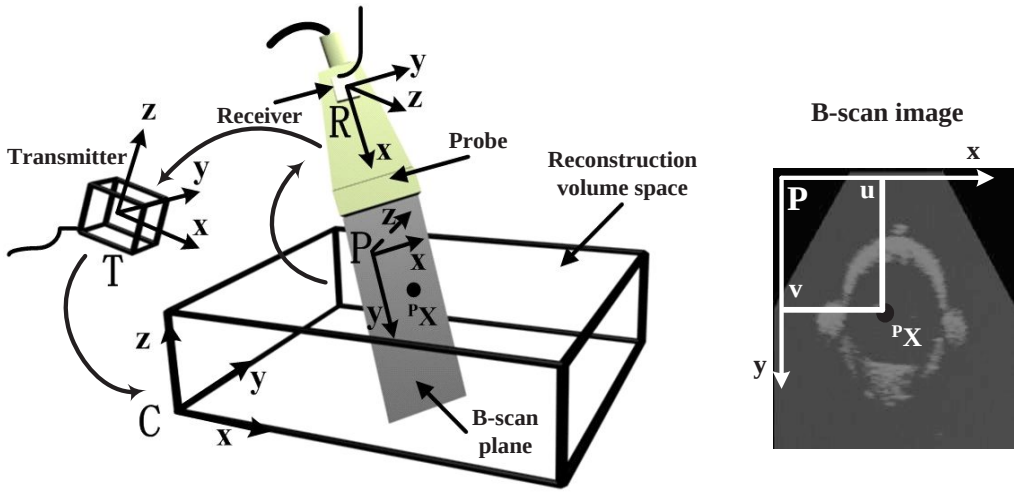

Figure 1. Coordinate systems relative to the volume reconstruction.

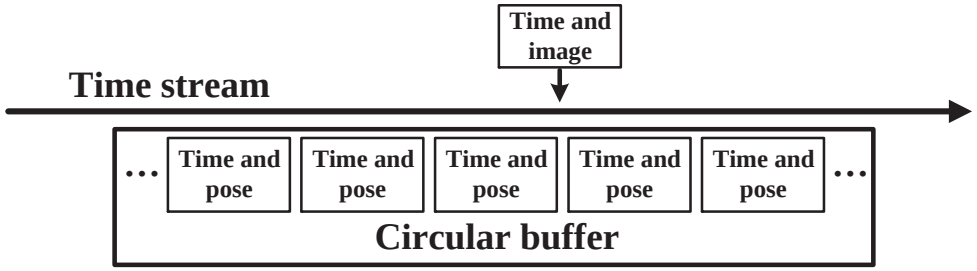

Figure 2. Interpolating the relative position and orientation of the latest image.

2.2 Real-time acquisition of images and positions

We employ a circular buffer with ten items, and three recurrent threads to acquire the latest B-scan image and its relative position and orientation. The ten latest readings acquired from the position sensor, with their relative time-stamps, are stored into the circular buffer circularly. The three threads are as follows:

- A position acquisition thread reads six-degree-of-freedom parameters from the position sensor continuously, and stores the readings, along with their calibrated time-stamps, into the circular buffer.
- An image acquisition thread obtains the latest B-scan image through the video frame grabber, and places the image, along with its calibrated time-stamp, into the memory.
- An interpolation thread interpolates the relative six-degree-of-freedom parameters of the latest image according to the time-stamps recorded by the above two threads (see Figure 2), and calculates the ${}^{T}T_{R}$ with the interpolated parameters.

This real-time acquisition technique is similar to the one described by Prager et al.[13]

2.3 Interactive selection of the ROI

Once the latest B-scan image and its relative ${}^{T}T_{R}$ are obtained, the four vertices of the image are transformed into the transmitter coordinate system by

$$ {}^{T}T_{P} = {}^{T}T_{R} \cdot {}^{R}T_{P}, {}^{T}X = {}^{T}T_{P} \cdot {}^{P}X, \tag{2} $$

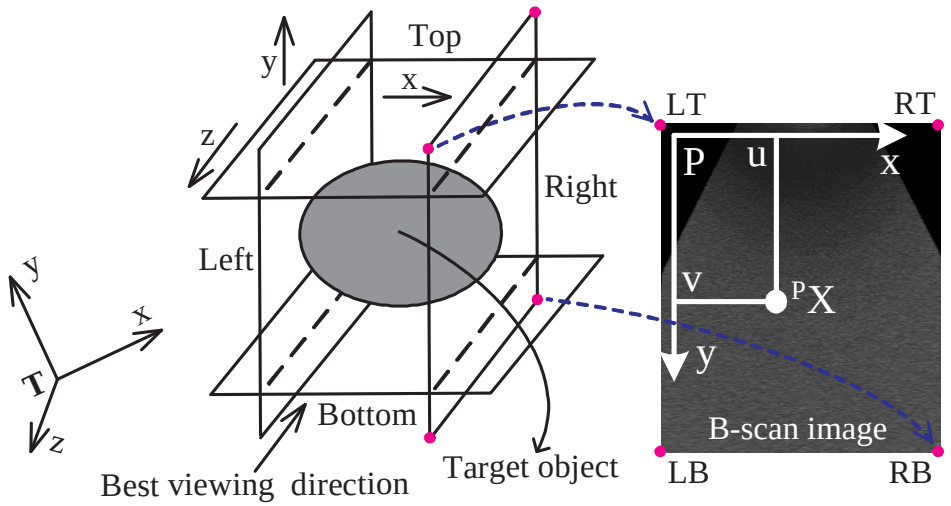

Figure 3. Interactive selection of the ROI.

and the image is then rendered in the transmitter coordinate system using the texture mapping of the OpenGL. To exhibit sufficient information about the tracked B-scan in the transmitter coordinate system, we employ multiple-view display (see Figure 6).

The multiple-view display updates the position and content of the tracked B-scan in the transmitter coordinate system in real time. Guided by the real-time feedbacks, we can explore the target object interactively to find its principal directions (x, y, and z) and the best viewing direction on the whole. Then four tracked B-scans that tightly enclose the target object are designated and recorded to decide the ROI. As shown in Figure 3, the four B-scans are designated in order of left, right, bottom and top. The left and right B-scans are approximately vertical to the principal direction x, while the bottom and top B-scans are approximately vertical to the principal direction y. Moreover, the four B-scans are basically along the principal direction z (the best viewing direction). For each B-scan, the coordinates of its four vertices in T, denoted as ${}^{T}X_{LT}$, ${}^{T}X_{LB}$, ${}^{T}X_{RB}$, and ${}^{T}X_{RT}$ respectively, are recorded. Then the center of the B-scan O is calculated by

$$O = ({}^{T}X_{LT} + {}^{T}X_{RB})/2, \tag{3}$$

and the normal of the B-scan N is calculated by

$$N = (({}^{T}X_{RT} - {}^{T}X_{LT})/ \parallel {}^{T}X_{RT} - {}^{T}X_{LT} \parallel) \otimes (({}^{T}X_{LB} - {}^{T}X_{LT})/ \parallel {}^{T}X_{LB} - {}^{T}X_{LT} \parallel), \tag{4}$$

where $\otimes$ denotes vector product, and $\parallel X \parallel$ means the modulus of the vector X.

2.4 Automatic determination of the reconstruction volume

With the recorded information of the four designated B-scans, the volume axes, axes origin, voxel size and volume size are figured out as follows.

2.4.1 Volume axes

As shown in Figure 4, assume O_L and O_R are the centers of the designated left and right B-scans respectively. N_{LR}, equal to $O_R - O_L$, is the vector from O_L to O_R. The normals of the designated left and right B-scans are N_L and N_R respectively. Provided N_L and N_{LR} are reverse, let N_L = -N_L. The same operation is performed on N_R. Then the x axis of the reconstruction volume is calculated by

$$N_x = (N_L + N_R)/ \parallel N_L + N_R \parallel . \tag{5}$$

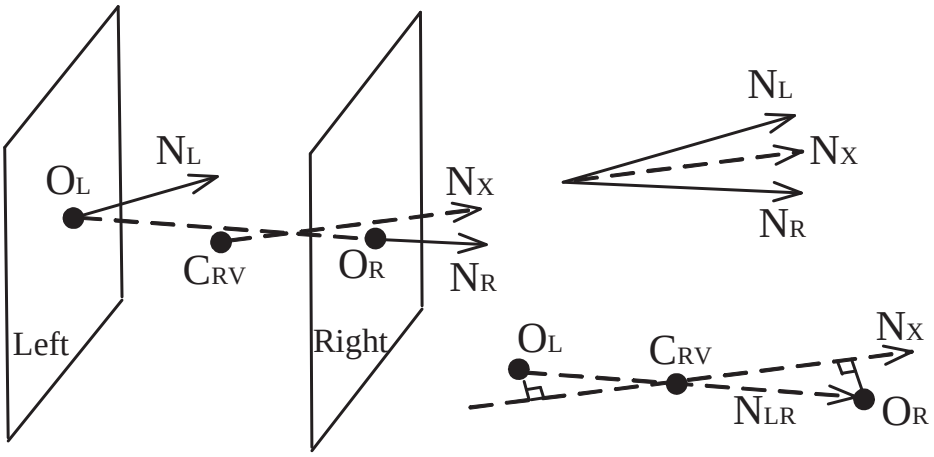

Figure 4. Automatic determination of the reconstruction volume.

Similarly, the y axis N_y can be figured out. The z axis N_z is defined by

$$N_z = N_x \otimes N_y. \tag{6}$$

Generally, the above N_x and N_y are not orthogonal. To ensure orthogonal axes, we adjust the N_y by

$$N_y = N_z \otimes N_x. \tag{7}$$

2.4.2 Volume axes origin

According to the N_{LR} and N_x, the volume extent along the x axis is calculated by

$$E_x = N_x \odot N_{LR}, \tag{8}$$

where $\odot$ denotes dot product. Similarly, the volume extent along the y axis, E_y, can be figured out. Assume the B-scan image size and pixel size are $W \times H$ and $S_x \times S_y$ respectively. Then the volume extent along the z axis, E_z, is defined by $E_z = H \cdot S_y$. Suppose C_{RV} is the center of the O_L, O_R, O_B, and O_T. Then the axes origin O_{RV} is calculated by

$$O_{RV} = C_{RV} - E_x \cdot N_x/2 - E_y \cdot N_y/2 - E_z \cdot N_z/2. \tag{9}$$

According to the volume axes and axes origin, the transformation matrix ${}^{C}T_T$ can be written as

$$\begin{bmatrix} N_x(x) & N_x(y) & N_x(z) & -N_x \odot O_{RV} \\ N_y(x) & N_y(y) & N_y(z) & -N_y \odot O_{RV} \\ N_z(x) & N_z(y) & N_z(z) & -N_z \odot O_{RV} \\ 0 & 0 & 0 & 1 \end{bmatrix}. \tag{10}$$

2.4.3 Voxel size and volume size

Taking the thickness of the ultrasound beam into account, each pixel in the B-scan image can be regarded as a small volume. We assume the thickness of the ultrasound beam is S_x (though generally the actual thickness is larger). Then the size of the pixel volume is $S_x \times S_x \times S_y$. During acquisition, ideally, the B-scan is made basically parallel to the best viewing direction (i.e., the z axis of the reconstruction volume) and approximately vertical to the scanning direction (e.g., the x axis of the reconstruction volume). However, generally there is an inevitable angle between the pixel volume and each axis while actual scanning. We take $\pi/4$ as a trade-off between reconstruction accuracy and efficiency, and define the voxel size as $V_x \times V_y \times V_z = S_x \cos(\pi/4) \times$

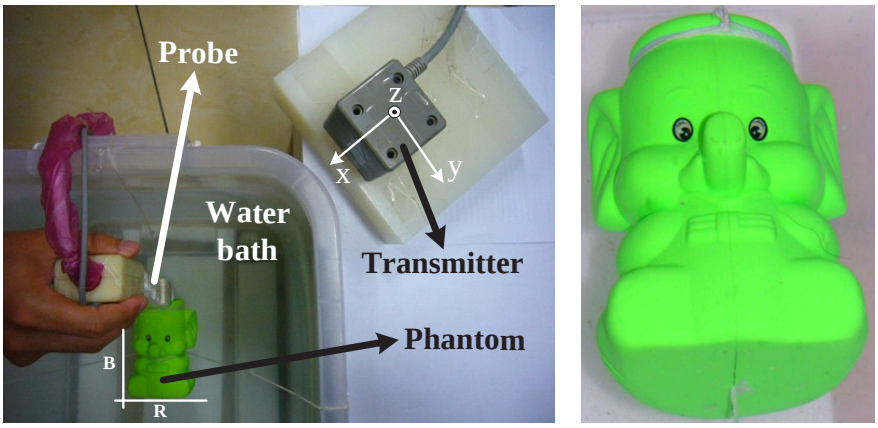

(a) Layout (b) Phantom

Figure 5. The experimental environment.

$S_x \cos(\pi/4) \times S_y \cos(\pi/4)$. Then the volume size can be calculated by

$$\begin{cases} L_x = [E_x/V_x + 0.5] \\ L_y = [E_y/V_y + 0.5] \\ L_z = [E_z/V_z + 0.5], \end{cases} \tag{11}$$

where [A] means the integer of the value A.

3. RESULTS

The proposed technique is integrated into a custom real-time freehand system. A WEUT-70X ultrasound scanner with a 3.5 MHz curved-array probe is used for B-scan acquisition. Output videos of the scanner are captured and digitized into discrete 2D images by a video frame grabber (OK_M10A). An electromagnetic position sensor (FASTRAK) is used to track the six-degree-of-freedom parameters of the probe. A Windows-PC with an Intel Core2 1.86 GHz processor and 1GB physical memory is the core of the system, which hosts the real-time freehand 3D ultrasound reconstruction software.

To evaluate the proposed technique, we perform 3D ultrasound reconstruction of a phantom with the freehand system. As shown in Figure 5(a), the phantom is hung in a water bath, and the transmitter is randomly placed aside. The latest B-scan image and recorded B-scan images can be exhibited in the transmitter coordinate system by the real-time multiple-view display, which can guide the exploration and ROI selection. After overview exploration of the phantom, we interactively designate four B-scans that are in the principal directions of the phantom to obtain a tightly enclosed ROI. The multiple-view display of the four recorded B-scans is shown in Figure 6. Immediately after the selection of the ROI, we get the ${}^{C}T_{T}$, voxel size, and volume size of the reconstruction volume, which are computed automatically by the freehand system. The detailed parameters are as follows.

$${}^{C}T_{T} = \begin{bmatrix} 0.560977 & 0.825374 & 0.0637398 & -108.925mm \\ -0.827259 & 0.556064 & 0.0802182 & 258.625mm \\ 0.0307666 & -0.0977299 & 0.994737 & 304.812mm \end{bmatrix}, \quad \begin{cases} V_x \times V_y \times V_z = 0.244 \times 0.244 \times 0.289mm^3 \\ L_x \times L_y \times L_z = 398 \times 381 \times 388 \end{cases}$$

With the parameters of the reconstruction volume, we use the technique described by Dai et al.[7] to perform real-time reconstruction of the phantom. The final reconstructed volume is visualized on a custom 3D medical image processing and analyzing platform (3DMed).[14] Figure 7 shows the splatting based[15] 3D visualization results of the reconstructed volume.

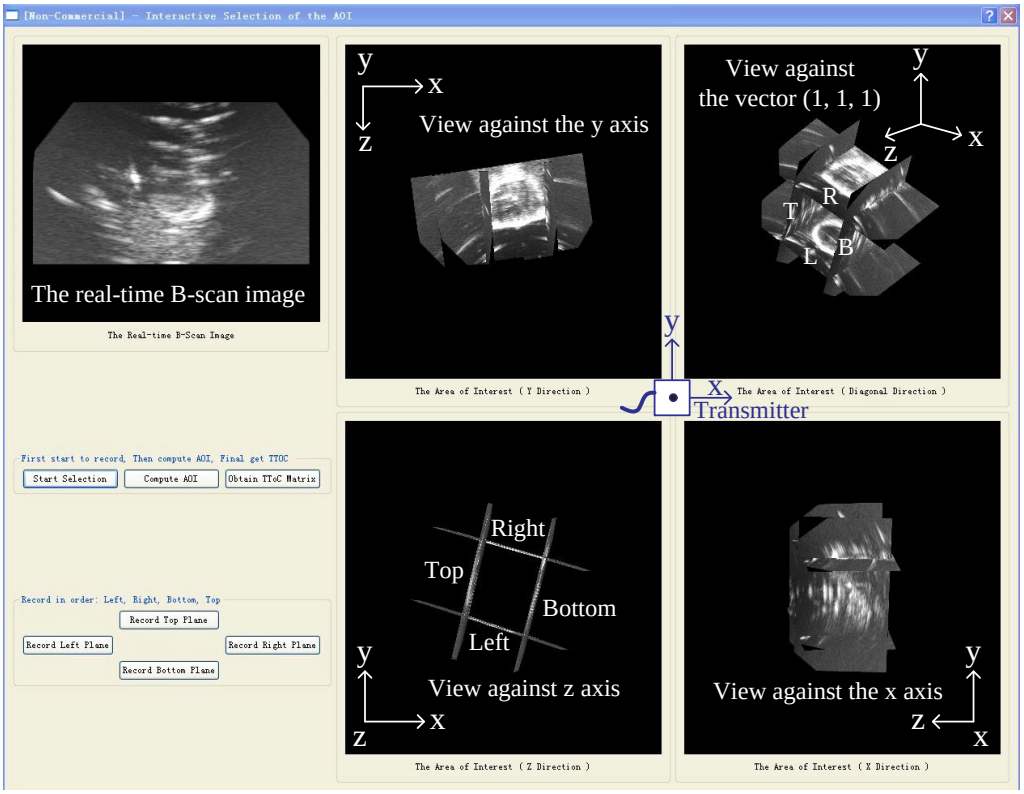

Figure 6. Real-time multiple-view display of the tracked B-scan images.

4. CONCLUSIONS

The determination of the reconstruction volume is a critical step for real-time freehand 3D ultrasound. This paper focuses on the point, and presents a semiautomatic technique to predetermine the reconstruction volume. The technique makes full use of the position and content of the tracked B-scan, as well as the interaction of the operator to select the ROI. The automatically determined reconstruction volume corresponding to the ROI is compact and aligned with the best viewing direction. The experimental results well demonstrate the validity of the technique.

The proposed technique can advance the efficiency and flexibility of a real-time freehand system. Furthermore, the technique is also useful for conventional freehand 3D ultrasound, where the technique can predetermine a compact reconstruction volume quickly, and the predetermined reconstruction volume can guide the scanning process for high quality acquisition. In the clinic, the examined area may be located at a pre-calibrated place for real-time reconstruction. Moreover, movements of the patient and transmitter may happen. The proposed technique allows the examined area to be placed at an arbitrary position and orientation. Furthermore, once a movement takes place, the reconstruction volume can be fast redetermined with the technique. This flexible and efficient nature makes the technique convenient for the clinician and comfortable for the patient.

ACKNOWLEDGMENTS

This work is supported by NBRPC (2006CB705700), PCSIRT (IRT0645), CAS HTP, CAS SREDP (YZ0642, YZ200766), JRFOCYS (30528027), NSFC (30672690, 30600151, 90209008, 60532050, 60621001, 30873462), BNSF (4071003) in China.

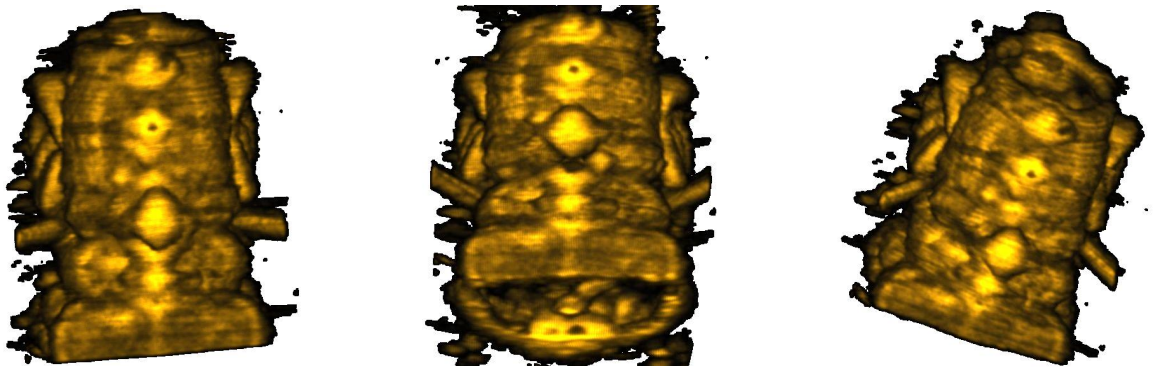

Figure 7. 3D visualization of the reconstructed volume with splatting.

REFERENCES

1. A. Gee, R. Prager, G. Treece, and L. Berman, "Engineering a freehand 3d ultrasound system," *Pattern Recognition Letters* **24**, pp. 757–777, 2003.
2. G. Unsgaard, S. Ommedal, T. Muller, A. Gronningsaeter, and T. A. N. Hernes, "Neuronavigation by intra-operative three-dimensional ultrasound: Initial experience during brain tumor resection," *Neurosurgery* **50**, pp. 804–812, 2002.
3. G. Unsgaard, O. M. Rygh, T. Selbekk, T. B. Muller, F. Kolstad, F. Lindseth, and T. A. N. Hernes, "Intra-operative 3d ultrasound in neurosurgery," *Acta Neurochir* **148**, pp. 235–253, 2006.
4. W. S. Edwards, C. Deforge, and Y. Kim, "Interactive three-dimensional ultrasound using a programmable multimedia processor," *International Journal of Imaging Systems and Technology* **9**(6), pp. 442–454, 1998.
5. J. N. Welch, J. A. Johnson, M. R. Bax, R. Badr, and R. Shahidi, "A real-time freehand 3-d ultrasound system for image-guided surgery," in *Proceedings of IEEE Ultrasound Symposium, San Juan, Puerto Rico: IEEE*, **2**, pp. 1061–1064, 2000.
6. D. G. Gobbi and T. M. Peters, "Interactive intra-operative 3d ultrasound reconstruction and visualization," in *Proceedings of Medical Image Computing and Computer Assisted Intervention (MICCAI), Tokyo, Japan: Springer*, **2489**, pp. 156–163, 2002.
7. Y. Dai, J. Tian, J. Xue, and J. Liu, "A qualitative and quantitative interaction technique for freehand 3d ultrasound imaging," in *Proceedings of IEEE Engineering in Medicine and Biology Society (EMBS), New York, USA: IEEE*, pp. 2750–2753, 2006.
8. C. D. Barry, C. P. Allott, N. W. John, P. M. Mellor, P. A. Arundel, D. S. Thomson, and J. C. Waterton, "Three dimensional freehand ultrasound: image reconstruction and volume analysis," *Ultrasound in Medicine & Biology* **23**(8), pp. 1209–1224, 1997.
9. R. S. José-Estépar, M. Martín-Fernández, P. P. Caballero-Martínez, C. Alberola-López, and J. Ruiz-Alzola, "A theoretical framework to three-dimensional ultrasound reconstruction from irregularly sampled data," *Ultrasound in Medicine & Biology* **29**(2), pp. 255–269, 2003.
10. D. G. Gobbi, B. H. K. Lee, and T. M. Peters, "Real-time 3d ultrasound for intra-operative surgical guidance," in *Proceedings of SPIE Medical Imaging, San Diego, CA, USA: SPIE*, **4319**, pp. 264–271, 2001.
11. O. V. Solberg, F. Lindseth, H. Torp, R. E. Blake, and T. A. N. Hernes, "Freehand 3d ultrasound reconstruction algorithms–a review," *Ultrasound in Medicine & Biology* **33**(7), pp. 991–1009, 2007.
12. R. W. Prager, R. N. Rohling, A. H. Gee, and L. Berman, "Rapid calibration for 3-d freehand ultrasound," *Ultrasound in Medicine & Biology* **24**(6), pp. 855–869, 1998.
13. R. W. Prager, A. Gee, and L. Berman, "Stradx: real-time acquisition and visualization of freehand three-dimensional ultrasound," *Medical Image Analysis* **3**(2), pp. 129–140, 1998.
14. J. Tian, J. Xue, Y. Dai, J. Chen, and J. Zheng, "A novel software platform for medical image processing and analyzing," *IEEE Transactions on Information Technology in Biomedicine* **12**(6), pp. 800–812, 2008.
15. M. Zwicker, H. Pfister, J. van Baar, and M. H. Gross, "Ewa splatting," *IEEE Transactions on Visualization and Computer Graphics* **8**(3), pp. 223–238, 2002.